

Uncoupling binding of substrate CO from turnover by vanadium nitrogenase

 HPSTAR
 157-2015

 Chi Chung Lee^a, Aaron W. Fay^a, Tsu-Chien Weng^{b,c}, Courtney M. Krest^b, Britt Hedman^b, Keith O. Hodgson^{b,d,1}, Yilin Hu^{a,1}, and Markus W. Ribbe^{a,e,1}
^aDepartment of Molecular Biology and Biochemistry, University of California, Irvine, CA 92697-3900; ^bStanford Synchrotron Radiation Lightsource, Stanford Linear Accelerator Center (SLAC) National Accelerator Laboratory, Stanford University, Menlo Park, CA 94025; ^cCenter for High Pressure Science & Technology Advanced Research, Shanghai 201203, China; ^dDepartment of Chemistry, Stanford University, Stanford, CA 94305; and ^eDepartment of Chemistry, University of California, Irvine, CA 92697-2025

Contributed by Keith O. Hodgson, October 5, 2015 (sent for review September 21, 2015; reviewed by Russ Hille and Douglas C. Rees)

Biocatalysis by nitrogenase, particularly the reduction of N₂ and CO by this enzyme, has tremendous significance in environment- and energy-related areas. Elucidation of the detailed mechanism of nitrogenase has been hampered by the inability to trap substrates or intermediates in a well-defined state. Here, we report the capture of substrate CO on the resting-state vanadium-nitrogenase in a catalytically competent conformation. The close resemblance of this active CO-bound conformation to the recently described structure of CO-inhibited molybdenum-nitrogenase points to the mechanistic relevance of sulfur displacement to the activation of iron sites in the cofactor for CO binding. Moreover, the ability of vanadium-nitrogenase to bind substrate in the resting-state uncouples substrate binding from subsequent turnover, providing a platform for generation of defined intermediate(s) of both CO and N₂ reduction.

nitrogenase | vanadium | carbon monoxide | turnover | substrate binding

Nitrogenases are complex metalloenzymes that catalyze the reduction of a variety of substrates under ambient conditions (1–3). Among them, two reactions bear significant relevance to environment- and energy-related areas: (i) the reduction of dinitrogen (N₂), a key element of nitrogen cycle in our biosphere, to the bio-accessible form of ammonia (NH₃); and (ii) the reduction of carbon monoxide (CO), a waste product from car and factory exhausts, to useful hydrocarbon products. The molybdenum (Mo)- and vanadium (V)-nitrogenases are two homologous members of this enzyme family. Both enzymes consist of a reductase component (*nifH*- or *vnfH*-encoded Fe protein) and a catalytic component (*nifDK*-encoded MoFe protein or *vnfDGG*-encoded VFe protein). Substrate turnover by both nitrogenases involves the formation of a functional complex between the two component proteins (1–3), which enables adenosine triphosphate (ATP)-dependent, interprotein transfer of electrons from the reductase component to the cofactor site of the catalytic component for the subsequent reduction of substrates.

Designated the M and V cluster, respectively, the cofactors of Mo- and V-nitrogenases closely resemble each other in geometry (3–7). Previous Fe K-edge X-ray absorption spectroscopy (XAS)/extended X-ray absorption fine structure (EXAFS) analysis revealed that the two cofactors had nearly indistinguishable metal-sulfur core structures, each comprising MFe₃S₃ (M = Mo or V) and Fe₄S₃ subclusters bridged by three μ₂-coordinated, belt-sulfur (S) atoms (Fig. 1*A* and *B*) (3, 6, 8). Recently, we performed a K-valence X-ray emission spectroscopy (XES) study of both protein-bound and solvent-extracted V clusters (Fig. 1*C*), which identified a carbide (C⁴⁻)-specific XES feature of the V cluster that was observed earlier in the case of the M cluster (9). Thus, the two cofactors not only share an overall homology in structure, but also have the same inner strengths that originate from the μ₆-coordinated interstitial carbide.

Surprisingly, despite the significant homology between their cofactors, the V- and Mo-nitrogenases differ in their reactivities

toward certain substrates; most notably, the V-nitrogenase is ~800-fold more active than its Mo counterpart in reducing CO to hydrocarbons (10, 11). The V-nitrogenase catalytically turns over CO as a substrate, generating 16.5 nmol reduced carbon/nmol protein/min; in contrast, the Mo-nitrogenase forms 0.02 nmol reduced carbon/nmol protein/min, which is far below the catalytic turnover rate. Such a discrepancy implies a difference between the redox potentials of the protein-bound V and M clusters, which could originate from a difference between the heterometal compositions (V vs. Mo) and/or electronic properties of the two cofactors, as well as a difference between the protein scaffolds that house these cofactors (VFe protein vs. MoFe protein). More importantly, it suggests redox-differentiated interactions of VFe and MoFe proteins with CO, which could be exploited to generate homologous CO-bound conformations of these two proteins for a joint mechanistic investigation of nitrogenase—an effort hampered by a lack of effective means to capture a catalytically relevant, substrate-bound conformation of this enzyme.

Results

Indeed, a homologous pair of CO-bound MoFe and VFe proteins can be generated at different redox states. In a recent study, a CO-bound form of MoFe protein was generated by incubating the MoFe protein with CO under turnover conditions. Subsequent crystallographic analysis of this CO-bound conformation

Significance

V-nitrogenase catalyzes two important reactions for environment- and energy-related areas: reduction of nitrogen to ammonia, and conversion of CO to hydrocarbons. The CO-bound conformation reported herein represents the first well-defined, substrate-bound nitrogenase with turnover capacity. Binding of CO to the resting-state V-nitrogenase uncouples CO binding from the subsequent turnover, which could facilitate capture of successive snapshots of CO reduction through controlled delivery of electron(s)/proton(s). The catalytic competence of this conformation suggests the mechanistic relevance of displacement of a belt-sulfur of the nitrogenase cofactor by a CO moiety upon binding, an event accommodated by the interstitial carbide that maintains the integrity of the cofactor while permitting a significant restructuring of the belt region that is crucial for substrate turnover.

Author contributions: C.C.L., B.H., K.O.H., Y.H., and M.W.R. designed research; C.C.L., A.W.F., T.-C.W., and C.M.K. performed research; C.C.L., T.-C.W., B.H., K.O.H., Y.H., and M.W.R. analyzed data; and K.O.H., Y.H., and M.W.R. wrote the paper.

Reviewers: R.H., University of California, Riverside; and D.C.R., Howard Hughes Medical Institute, Caltech.

The authors declare no conflict of interest.

¹To whom correspondence may be addressed. Email: hodgsonk@stanford.edu, yilinh@uci.edu, or mribbe@uci.edu.

This article contains supporting information online at www.pnas.org/lookup/suppl/doi:10.1073/pnas.1519696112/-DCSupplemental.

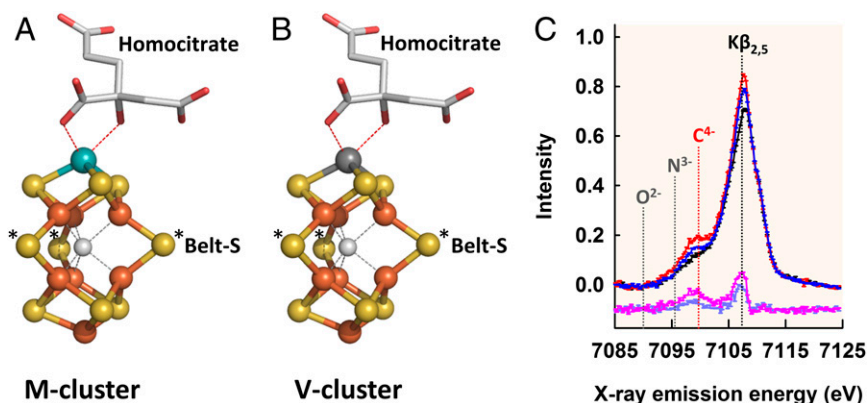


Fig. 1. Structural homology between M and V clusters. Structural models of the M (A) and V (B) clusters. Protein Data Bank (PDB) 3U7Q (7), XAS/EXAFS (8), and XES (this study) data were used to generate these models. Atoms are colored as follows: Fe, orange; S, yellow; Mo, cyan; O, red; C, light gray; V, dark gray. (C) K-valence XES spectra of V cluster (Top, red), holo VFe protein (Top, blue), and apo VFe protein (Top, black); and difference spectra (offset for clarity) of V cluster/apo-VFe protein (Bottom, magenta) and holo-apo-VFe protein (Bottom, gray/blue). The dashed lines denote the calculated energy positions for M clusters containing interstitial C^4 , N^3 , and O^{2-} , respectively, relative to the $K\beta_{2,5}$ line (9).

clearly revealed that a CO moiety took the place of one belt-S and assumed a μ_2 coordination between two Fe atoms across the belt of the M cluster, an astonishing observation that led to the proposal that a reactive iron species was formed upon displacement of sulfur to accommodate the binding of CO (Fig. 2A) (12). Electron paramagnetic resonance (EPR) analysis of this CO-bound MoFe protein identified a CO-derived signal (Fig. 2C) that was nearly identical to a previously observed lo-CO signal (Fig. S14) that emerged upon incubation of MoFe protein with CO under turnover conditions (13, 14). ENDOR analysis of the lo-CO conformation led to the suggestion that a single CO was bridged or semibridged between two cross-belt Fe atoms in a manner similar to that observed in the recent crystal structure, although the belt-S remained intact in this proposed model (Fig. S1B) (15, 16). Interestingly, incubation of the dithionite-reduced, resting-state VFe protein with 100% CO resulted in the appearance of a small, yet distinct, CO-originated EPR signal (Fig. 2D) that was highly analogous to that displayed by the CO-bound MoFe protein (Fig. 2C). The striking similarity between the line shapes of these signals points to a close resemblance between the two CO-bound conformations (Fig. 2A vs. B), particularly given the structural/functional homology between the V and M clusters (Fig. 1). Perhaps more excitingly, it suggests the possibility to use VFe protein as an effective tool to establish the catalytic relevance of these homologous CO-bound conformations, a major hurdle for MoFe protein-based work due to an extremely poor efficiency of this protein to turn over CO upon binding.

To explore the utility of VFe protein in generating turnover-related CO-bound conformation, the resting-state VFe protein was incubated with or without 100% CO in the presence of dithionite ($E^{0'} = -0.66$ V) (17), europium (II) ethylene-glycol-tetraacetic-acid (Eu^{II} -EGTA; $E^{0'} = -0.88$ V) (17), and europium (II) diethylene-triamine-pentaacetic-acid (Eu^{II} -DTPA; $E^{0'} = -1.14$ V) (17), respectively, and subsequently reisolated into a reductant-free buffer under Ar (Fig. S2). EPR analysis revealed that the CO-originated signal not only was retained by the VFe protein upon reisolation from the CO atmosphere, but also displayed an increase in intensity when the VFe protein was treated with reductants of increasing strengths (i.e., dithionite < Eu^{II} -EGTA < Eu^{II} -DTPA) during the process of CO loading) (Fig. 3A and Fig. S3B). Consistent with this observation, when these reisolated VFe proteins were treated with an oxidant, indigo disulfonate (IDS; $E^{0'} = -0.125$ V) (18), they released CO in amounts that corresponded to occupancies of 0.07, 0.57, and 0.91 mol CO/mole protein, respectively, in samples treated with

dithionite, Eu^{II} -EGTA and Eu^{II} -DTPA (Fig. 3B, red bars). Strikingly, the signal intensities of these samples displayed a linear correlation with the amounts of CO released from them (Fig. 3C), firmly establishing CO as the origin of the unique EPR

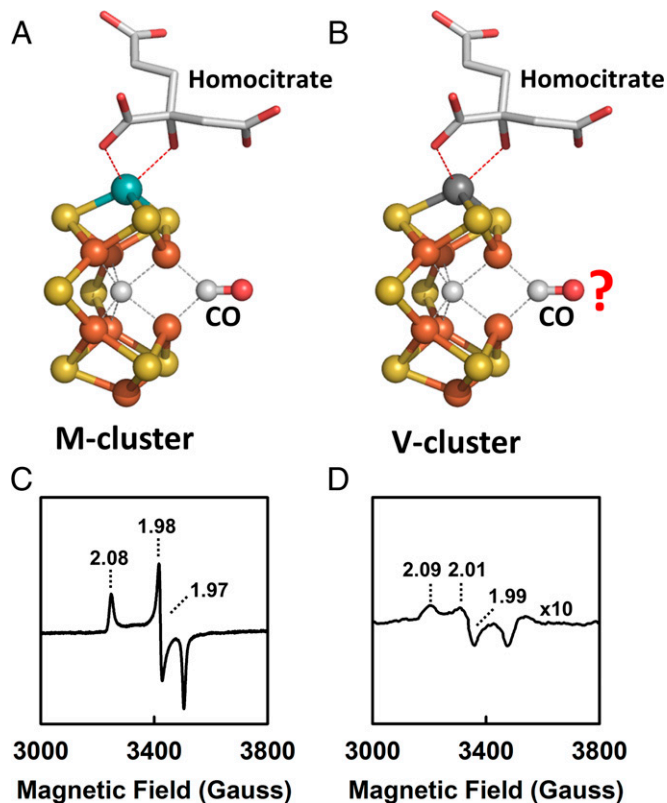


Fig. 2. Homologous conformations of CO-bound M and V clusters. Crystal structure of CO-bound M cluster (A) and homologous model of CO-bound V cluster (B). PDB 4TKV (12), XAS/EXAFS (8), and XES (this study) data were used to generate these models. Atoms are colored as in Fig. 1. EPR features of the CO-bound MoFe (C) and VFe (D) proteins were generated under turnover and resting-state conditions, respectively. Shown are difference spectra of samples prepared in the presence and absence of CO. Spectra were collected in perpendicular mode at 10 K (C) and 30 K (D). The g values are indicated.

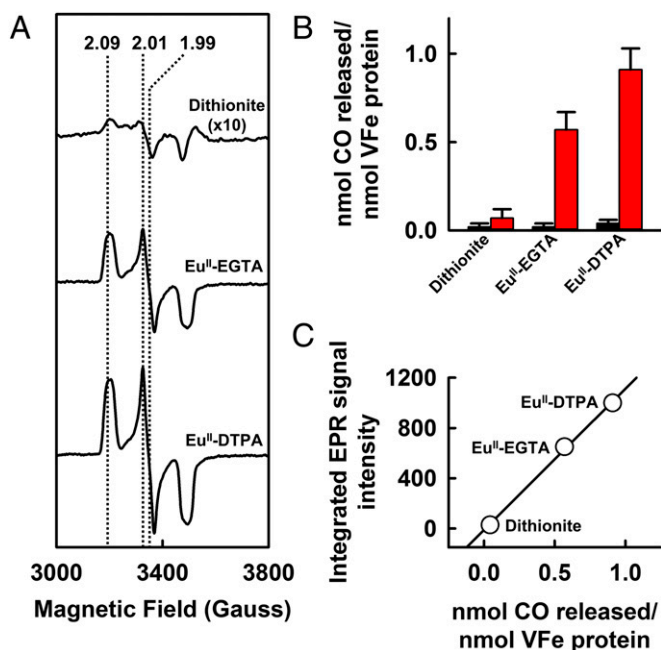


Fig. 3. Loading of CO onto the resting-state VFe protein. (A) EPR features of CO-bound VFe proteins prepared in the presence of dithionite, Eu^{II}-EGTA, and Eu^{II}-DTPA, respectively. Shown are difference spectra of samples prepared in the presence and absence of CO (Fig. S3). Spectra were collected in perpendicular mode at 30 K. The *g* values are indicated. (B) Release of CO from preloaded VFe proteins (same as those in A) upon addition of dithionite (black bars) and IDS (red bars). (C) Correlation between EPR signal intensities (data taken from A) and CO release (data taken from B).

signal and demonstrating a redox dependence of CO binding to the VFe protein. The observation of a high CO occupancy in the Eu^{II}-DTPA-treated VFe protein was particularly important, as it paved the way for the subsequent examination of the catalytic competence of the CO-bound conformation of VFe protein.

To carry out experiments on the catalytic competence of the CO-bound conformations, the VFe protein was loaded with ¹²CO or ¹³CO in the presence of Eu^{II}-DTPA, reisolated from the CO atmosphere, and subjected to turnover conditions upon addition of Fe protein and ATP in the presence of dithionite. EPR analysis revealed that the VFe protein preloaded with ¹²CO (Fig. S4, trace 1) displayed a signal upon turnover (Fig. S4, trace 2) that was highly similar to that displayed by the unloaded VFe protein upon direct turnover of ¹²CO (Fig. S4, trace 3). Gas chromatograph-mass spectrometry (GC-MS) analysis further demonstrated that the VFe protein-bound ¹³CO could be fully reduced in the absence of extra CO, resulting in the formation of ¹³CH₄ (Fig. 4A) and ¹³CD₄ (Fig. 4B), respectively, as the turnover products in H₂O- and D₂O-based reactions. In the presence of 1% extra ¹²CO, however, the VFe protein-bound ¹³CO could also undergo reductive C-C coupling, leading to the formation of ¹³CH₂=¹²CH₂ (Fig. 4C) and ¹³CH₃-¹²CH₃ (Fig. 4D) as additional turnover products in the H₂O-based reaction. The observation of a fully deuterated C1 product (i.e., ¹³CD₄) suggests that the CO moiety does not undergo further reduction upon binding, which provides additional support to the proposed resemblance between the CO-bound V and M clusters (Fig. 2 A and B); whereas the formation of ¹³C/¹²C-mixed C2 products not only reaffirms the capture of a singular ¹³CO entity on the V cluster, but also illustrates the full catalytic range of this CO-bound conformation in undergoing CO reduction and/or reductive C-C coupling.

Discussion

The CO-bound conformation reported here represents, to our knowledge, the first well-defined, substrate-bound nitrogenase with turnover capacity. Loading of CO onto the resting-state VFe protein effectively uncouples CO binding from the subsequent turnover events, which could facilitate development of redox-dependent strategies for controlled delivery of electron(s)/proton(s) to the CO-bound species to capture successive snapshots along the reaction pathway of CO reduction. Moreover, similar strategies may be used to trap other substrates, such as N₂, on the VFe protein, which will provide the long-sought-after answer to the question of how nitrogenase works with its physiological substrate. As for N₂ vs. CO, one cannot help but note the respective parallelism between the nitrogenase-based CO and N₂ reduction and industrial Fischer-Tropsch and Haber-Bosch process, which is interesting from a biotechnological perspective. Additionally, certain analogies between the two nitrogenase-catalyzed reactions cannot be overlooked, particularly given that CO and N₂ are isoelectronic molecules that compete with each other for interaction with cofactor. Thus, the utility of studies of CO reduction by nitrogenase—a biological setting where Fischer-Tropsch meet Haber-Bosch—in our quest for a mechanistic understanding of nitrogenase can be duly anticipated.

Fortunately, such a quest has already had an excellent start, owing a great deal to the recent crystal structure of CO-bound MoFe protein (12). Despite the fact that the CO-bound MoFe protein is hardly capable of turnover (and hence the designation CO-inhibited MoFe protein), its close resemblance to the CO-bound VFe protein renders it highly relevant to the catalytic turnover of CO. The observation of displacement of a belt-S by a CO moiety in this conformation unveils an unprecedented mechanism of CO binding that relies on a substantial rearrangement of the belt-S to expose and activate the two Fe sites for the initial CO binding and, possibly, the subsequent attachment of additional CO moieties for C-C coupling. The flexibility of the cofactor belt is likely accommodated by the presence of carbide in the central cavities of both M and V clusters (Fig. 1), which provides a strong anchor for the reactive Fe sites during

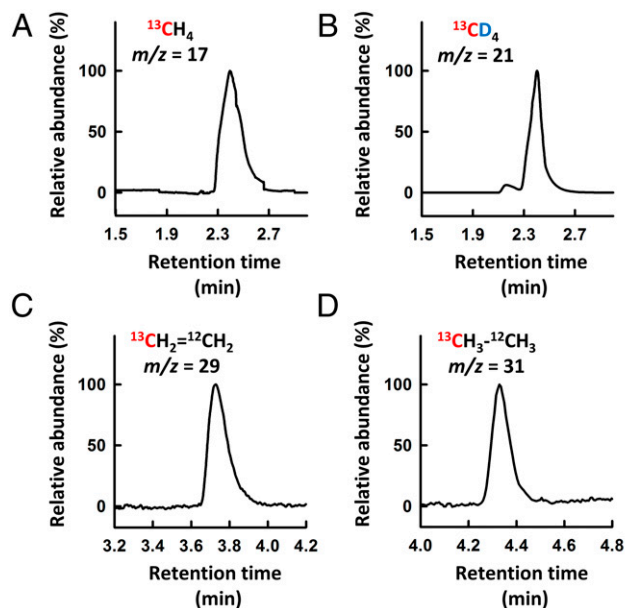


Fig. 4. Catalytic competence of CO-bound VFe protein. GC-MS analysis of products formed upon turnover of the ¹³CO-bound VFe protein in H₂O (A)- and D₂O (B)-based reactions without extra CO or in an H₂O-based reaction with 1% extra ¹²CO (C and D).

ligand exchange, thereby maintaining the integrity of the co-factor while permitting a significant restructuring of the belt that is crucial for substrate turnover. Although details of this reaction require further investigation, the ongoing and future structural and biochemical analyses of turnover-related conformations of the homologous nitrogenases promise to bring more excitement and provide previously unidentified insights into the reaction mechanism of this fascinating enzyme.

Materials and Methods

Unless otherwise specified, all chemicals were purchased from Sigma-Aldrich. Natural abundance ^{12}C (99.5% purity) was purchased from Praxair. All isotope-labeled compounds ($\geq 98\%$ isotopic purity) were purchased from Cambridge Isotopes.

Cell Growth and Protein Purification. *Azotobacter vinelandii* strains expressing His-tagged MoFe protein, His-tagged holo- and apo-VFe proteins, and nontagged *vnfH*- and *nifH*-encoded Fe proteins were grown as described elsewhere (19). Published methods were used for the purification of these nitrogenase proteins (19).

Trapping CO on MoFe Protein Under Turnover Conditions. Samples were prepared according to the published method that was used to generate a CO-bound form of MoFe protein for crystallographic analysis (12). In short, the MoFe protein was equilibrated with 100% (or 1 atm) CO before replacement of 10% headspace by an equal volume of C_2H_2 . Subsequently, 30 mg MoFe protein was combined with a twofold molar excess of *nifH*-encoded Fe protein in a 5-mL reaction mixture containing 6 mM Na_2ATP , 8 mM MgCl_2 , 50 mM phosphocreatine, 0.20 mg/mL creatine phosphokinase, 20 mM dithionite ($\text{Na}_2\text{S}_2\text{O}_4$), and 25 mM Tris-HCl (pH 8.0). The mixture was stirred for 10 min before the MoFe protein was reisolated under an overpressure of 16 psi CO in an Amicon ultrafiltration cell by a membrane with a molecular weight cutoff of 100,000 Da. An equal volume of buffer containing 20 mM $\text{Na}_2\text{S}_2\text{O}_4$ and 25 mM Tris-HCl (pH 8.0) was added after concentration to remove the Fe protein. The reisolated MoFe sample was then transferred into a sealed vial containing 10% CO and allowed to sit at room temperature for 2.5 h before it was transferred into an EPR tube and frozen in liquid nitrogen (LN_2).

Trapping CO on VFe Protein in Resting State Using Different Reductants. Stock solutions of Eu^{II} -EGTA and Eu^{II} -DTPA were prepared as described previously (20, 21). The dithionite-reduced VFe protein was passed through a G25 column in a buffer containing 25 mM Tris-HCl (pH 8.0) and 500 mM NaCl to remove excess dithionite before exposure to 100% CO. Immediately following this step, Eu^{II} -EGTA or Eu^{II} -DTPA was added at a final concentration of 20 mM to a 2-mL solution containing 40 mg VFe protein, and the mixture was stirred for 20 min at room temperature. To remove trace CO (which was dissolved in solution) and the Eu^{II} reductants (which would display strong, interfering EPR signals), the reductant-treated VFe protein was reisolated by a Ni-NTA column (GE Healthcare) on which the His-tagged VFe protein was immobilized before it was washed with several column volumes of an anaerobic, reductant-free buffer containing 500 mM NaCl, 10% (vol/vol) glycerol, and 25 mM Tris-HCl (pH 8.0) and eluted with the same buffer containing 250 mM imidazole. The reisolated, CO-bound VFe protein samples were kept in a sealed vial under Ar atmosphere and subsequently examined for CO release, turnover products, and EPR properties (see below for details).

Analysis of CO Release from the CO-Bound VFe protein. CO was determined by headspace analysis using a Thermo Trace 1300 GC-FID instrument, which had its detector interfaced with a methanizer (Thermo Electron North America). CO in the headspace was separated on a TG-BOND Msieve 5A column (30 m \times 0.32 mm ID \times 30 μm film) (Thermo Electron North America), hydrogenated at the methanizer, and subsequently detected by the FID. The headspace of each 5-mg reisolated, CO-bound VFe protein sample (see above) was first checked for background CO level and then treated by either 40 mM dithionite or 5 mM IDS to release protein-bound CO. The sample was then allowed to sit for 30 min at room temperature before its headspace was analyzed for the amount of CO that was released from the VFe protein.

Determination of Product Formation by the CO-Bound VFe Protein Upon Turnover. The reisolated, ^{13}C -bound VFe protein samples were generated in the presence of Eu^{II} -DTPA (see above). Subsequently, ~ 30 mg of the

thus-prepared VFe protein was combined with a 10-fold molar excess of *vnfH*-encoded Fe protein in a 2.5-mL reaction mixture containing 20.4 mM Na_2ATP , 43.2 mM MgCl_2 , 245 mM creatine phosphate, 420 U/mL creatine phosphokinase, and 25 mM Tris-HCl (pH 8.0) and incubated at 30 $^\circ\text{C}$ for 3 h either under Ar (i.e., without extra CO) or in the presence of 1% extra ^{13}C to allow turnover of the protein-bound ^{13}C . In addition, using a centrifugal filter unit with a molecular weight cutoff of 50,000 Da, the ^{13}C -bound VFe protein sample was also exchanged into a D_2O -based buffer containing the same reaction components in 50 mM (D11)-Tris [i.e., $(\text{DOCD}_2)_3\text{CND}_2$] (pH 8.0) before it was subjected to turnover conditions as described above. Product formation was then determined by analyzing the headspace of each sample by GC-MS as described earlier (22).

EPR Spectroscopy. All EPR samples were prepared in a Vacuum Atmospheres dry box at an oxygen level of < 4 ppm. The CO-bound, resting-state VFe protein samples were prepared in the presence of dithionite or Eu^{II} reductants and reisolated into an anaerobic, reductant-free buffer under Ar (see above). The CO-turnover samples were prepared by either directly combining 15 mg VFe protein and 0.8 mg *vnfH*-encoded Fe protein in a 1-mL reaction mixture containing 6 mM Na_2ATP , 8 mM MgCl_2 , 50 mM phosphocreatine, 0.20 mg/mL creatine phosphokinase, 20 mM $\text{Na}_2\text{S}_2\text{O}_4$, and 25 mM Tris-HCl (pH 8.0) (14, 23) or by first generating the ^{13}C -bound VFe protein sample and subsequently combining it with the same reaction mixture above. All samples were frozen in LN_2 and analyzed by a Bruker ESP 300 Ez spectrophotometer (Bruker) interfaced with an Oxford Instruments ESR-9002 liquid helium continuous-flow cryostat. A total of five scans were recorded for each sample at 10 or 30 K in perpendicular mode using a microwave power of 50 mW, a gain of 5×10^4 , a modulation frequency of 100 kHz, a modulation amplitude of 5 G, and a microwave frequency of 9.62. Spin quantitation of EPR signals was carried out as described elsewhere (19, 24).

XES Spectroscopy. The V cluster (extracted into *N*-methyl formamide) and the holo- and apo-VFe proteins were prepared as described previously (8). All XES samples were ~ 2 mM in protein concentration, which corresponded to a Fe concentration of ~ 14 – 30 mM. Samples were anaerobically loaded into Delrin XAS cells with 38- μm Kapton windows and immediately frozen in pentane slush. All X-ray emission spectra were collected at Stanford Synchrotron Radiation Lightsource Beam Line 6-2b. A Rh-coated mirror before the Si(111) double-crystal monochromator was used to collimate the beam and reject high-order harmonics. The X-ray energy was calibrated using Fe K-edge absorption spectra from a Fe foil, with the first inflection point assigned to 7112.0 eV. The X-ray beam was focused with a Rh-coated parabolic mirror with a spot size of 0.4 mm (fwhm, H) by 0.28 mm (fwhm, V) on the sample. The full photon flux on the samples was 1×10^{13} ph/s at 7,800 eV. Fe X-ray emission spectra were collected with the incident X-ray energy at 7,800 eV. Six 1-m spherically bent Ge(620) crystal analyzers were used to resolve the X-ray fluorescence, with an energy bandwidth of 0.84 eV, and focused on a silicon drift diode detector, located below the sample in a vertical Rowland geometry. A polyethylene bag (25- μm thickness) was filled with helium and placed in between the sample, the crystal analyzers, and the detector to minimize attenuation of the fluorescence signal due to air absorption. The XES spectra were measured with the samples maintained at 13–15 K in a continuous-flow liquid helium cryostat. Radiation-damage assessment was performed on each sample before the XES measurements to determine the required X-ray attenuation (100–125 μm Al filter depending on the sample) and the corresponding exposure time on one fresh spot. Each XES spectrum was collected on multiple fresh spots to avoid X-ray-induced photo-reduction. X-ray emission spectra were collected from 7,030 to 7,080 eV for the Fe $\text{K}\beta$ region and from 7,075 to 7,125 eV for the Fe K-valence region, with an increment of 0.25 eV and a count time of 1 s at each point. For the isolated V cluster and holo- and apo-VFe protein samples, 5/4/4 $\text{K}\beta$ scans and 105/102/88 K-valence scans were recorded, merged, normalized to the incident photo flux, and further normalized to the total integrated area of the full spectra. For the K-valence emission region, the background tail from the $\text{K}\beta$ main line and beyond the K-valence region were fit with a second-order polynomial.

ACKNOWLEDGMENTS. We thank K. Tanifuji, J. G. Rebelein, and D. Sokaras for technical and experimental support. This work was supported by NIH Grants R01 GM67626 (to M.W.R.) and P41GM103393 (to K.O.H.). Stanford Synchrotron Radiation Lightsource (SSRL) operations are funded by the Department of Energy (DOE) Basic Energy Sciences and the SSRL Structural Molecular Biology Program is funded by NIH National Institute of General Medical Sciences P41GM103393 and DOE Basic Environmental Research.

